Pharmacological Research 167 (2021) 105545

Contents lists available at ScienceDirect

Pharmacological Research

journal homepage: www.elsevier.com/locate/yphrs

Palmitoylethanolamide and hemp oil extract exert synergistic anti-nociceptive effects in mouse models of acute and chronic pain

Alex Mabou Tagne [a,1], Yannick Fotio [a,1], Lin Lin [a], Erica Squire [a], Faizy Ahmed [a], Tarif Ibne Rashid [a], Elnaz Karimian Azari [b], Daniele Piomelli [a,c,d,*]

[a] Department of Anatomy and Neurobiology, University of California, Irvine, CA 92697-4625, USA
[b] Metagenics, Aliso Viejo, CA 92656, USA
[c] Department of Biological Chemistry, University of California, Irvine, CA 92697-4625, USA
[d] Department of Pharmaceutical Sciences, University of California, Irvine, CA 92697-4625, USA

ARTICLE INFO

Keywords:
Palmitoylethanolamide
Hemp
Acute pain
Chronic pain

ABSTRACT

The use of products derived from hemp – i.e., cannabis varieties with low Δ^9-tetrahydrocannabinol (Δ^9-THC) content – as self-medication for pain and other health conditions is gaining in popularity but preclinical and clinical evidence for their effectiveness remains very limited. In the present study, we assessed the efficacy of a full-spectrum hemp oil extract (HOE; 10, 50 and 100 mg-kg^{-1}; oral route), alone or in combination with the anti-inflammatory and analgesic agent palmitoylethanolamide (PEA; 10, 30, 100 and 300 mg-kg^{-1}; oral route), in the formalin and chronic constriction injury (CCI) tests. We found that HOE exerts modest antinociceptive effects when administered alone, whereas the combination of sub-effective oral doses of HOE and PEA produces a substantial greater-than-additive alleviation of pain-related behaviors. Transcription of interleukin (IL)−6 and IL-10 increased significantly in lumbar spinal cord tissue on day 7 after CCI surgery, an effect that was attenuated to the same extent by HOE alone or by the HOE/PEA combination. Pharmacokinetic experiments show that co-administration of HOE enhances and prolongs systemic exposure to PEA. Collectively, our studies lend support to possible beneficial effects of using HOE in combination with PEA to treat acute and chronic pain.

1. Introduction

Current pain management strategies rely on three main classes of drugs: opioids, gabapentinoids and non-steroidal anti-inflammatory agents. These medications are widely used in clinical practice but produce adequate pain relief only in a fraction of patients who take them. In addition, their use is associated with dose-limiting side effects, such as tolerance, abuse liability and gastrointestinal toxicity. Thus, despite important progress in charting the mechanisms that underpin pathological pain, there is still an unmet need for safe and effective analgesic therapies [44].

A recent survey by the National Academies of Sciences, Engineering and Medicine (NASEM) concluded that substantial clinical evidence indicates that cannabis and cannabinoids are effective in the treatment of chronic pain in adults [30]. This statement is supported by a large number of preclinical studies which point to Δ^9-tetrahydrocannabinol (Δ^9-THC) as the compound that most likely underpins the analgesic properties of cannabis [46]. Δ^9-THC and its synthetic mimics exert a broad spectrum of antinociceptive effects in animal models by engaging G protein-coupled CB_1 and CB_2 cannabinoid receptors [42]. CB_1 receptors are highly expressed in pain-processing structures of the peripheral and central nervous systems as well in non-neural cells throughout the body, while CB_2 receptors are primarily concentrated in cells of the innate and adaptive immune systems [25]. The presence of CB_1 in brain areas involved in the control of mood, reward and cognition underlies the psychotropic properties of Δ^9-THC, which limit the use of this agent in pain therapy [32].

In addition to Δ^9-THC, cannabis contains more than 140 phytochemicals that share a similar terpenophenolic nucleus but do not productively interact with either CB_1 or CB_2 receptors. There is evidence that one such compound, cannabidiol (CBD), might reduce pain without causing intoxication but its analgesic efficacy and mechanism remain

* Correspondence to: Louise Turner Arnold Chair in the Neurosciences Distinguished Professor, Departments of Anatomy and Neurobiology, Pharmaceutical Sciences and Biological Chemistry Director, Center for the Study of Cannabis University of California, Irvine 92697-1275, USA.
E-mail address: piomelli@hs.uci.edu (D. Piomelli).
[1] Equal contribution

https://doi.org/10.1016/j.phrs.2021.105545
Received 21 January 2021; Received in revised form 8 March 2021; Accepted 9 March 2021
Available online 12 March 2021
1043-6618/© 2021 Elsevier Ltd. All rights reserved.

unclear [9,11]. Cannabis contains other non-psychotropic cannabinoid and terpene molecules, whose contribution to the analgesic properties of the plant may be far from negligible [17,37]. Indeed, cannabis varieties that contain less than 0.3% Δ^9-THC – conventionally referred to as 'hemp' – are becoming increasingly popular as self-medication for pain and other health conditions, and the enactment of the U.S. 2018 Farm Bill, which effectively legalized the cultivation and sale of hemp, has only increased this popularity. However, we still know surprisingly little about the effectiveness of hemp-based products on pain.

Palmitoylethanolamide (PEA) belongs to the fatty acid ethanolamide (also known as N-fatty acylethanolamine) class of signaling lipids, which also includes the endocannabinoid anandamide and the satiety factor oleoylethanolamide [33]. A large body of animal and human studies indicate that PEA produces safe and effective analgesia [16,19,23,31,6], which depends on the compound's ability to engage the nuclear receptor peroxisome proliferator-activated receptor-α (PPAR-α) [23,24].

In the present study, we investigated the efficacy of a full-spectrum hemp oil extract (HOE), either alone or in combination with PEA, in two mouse models of acute and chronic pain: the formalin and the chronic-constriction injury tests. The results show that HOE exerts modest antinociceptive effects when administered alone, whereas the combination of HOE with PEA results in a substantial alleviation of pain-related behaviors. Pharmacokinetic studies show that this unexpected synergistic interaction may be accounted for, at least in part, by the ability of HOE to prolong the exposure and lifetime of PEA in circulation.

2. Materials and methods

2.1. Animals

We used male CD-1 mice (9–10 weeks old; Charles River, Wilmington, MA, US) weighing 25–30 g upon arrival. They were randomly assigned to treatment groups and housed in ventilated plastic cages (4–5 per cage) in the animal facility of the University of California, Irvine. Animals were maintained in a pathogen-free environment (12-h light/dark cycle) under controlled temperature (20 ± 2 °C) and humidity (55–60%) with food and water available ad libitum. Mice were allowed to acclimate for at least 7 days and experiments were conducted during the light phase of the light/dark cycle. All efforts were made to minimize the number of animals used and their discomfort. All procedures were approved by the Institutional Animal Care and Use Committee at the University of California, Irvine, and were carried out in strict accordance with the National Institutes of Health guidelines for the care and use of animals.

2.2. Test compounds preparation and administration

HOE (code: VOHO-MGC) and PEA (batch n°20190604_03) were supplied by Metagenics (https://www.metagenics.com) at no charge. The chemical composition of HOE is presented in Table 1 and the certificate of analysis is shown as Supporting information. The extract was aliquoted upon arrival at our facility and kept at −80 °C until use. Before tests, aliquots were thawed at room temperature and the extract was diluted to the desired dose in a vehicle of 85% distilled water/15% Tween 80. Defrosted samples were discarded after use. HOE was subjected to an internal quality control to monitor its content of CBD and CBDA over time. The results are shown in Table 2. HOE, PEA and their combinations were administered in volumes of 10 mL/kg by oral gavage.

2.3. Formalin test

The formalin test was described in detail previously [13]. We injected formalin (1% v/v, 10 μL) or vehicle (saline, 10 μL) into the plantar surface of the right hind paw of male mice. Test compounds or vehicle (85% distilled water/15% Tween 80) were administered orally 1 h before formalin injection. Following injection, mice were immediately transferred to a transparent observation chamber where nocifensive behavior (time spent licking or biting the injected paw, number of shakings) was continuously recorded by a video camera for 60 min and then measured by trained observers blinded to experimental conditions. Behavioral tests and paw edema measurements were performed on post-formalin day (PFD) 7 in both the injected (ipsilateral) and contralateral paws.

Table 1
Chemical composition of hemp oil extract. Nd-Not detected = less than 0.01% g/g.

Phytochemical	% g/g
Cannabidivarin (CBDV)	nd
Cannabidiolic acid (CBDA)	1.43
Cannabigerol (CBG)	nd
Cannabigerolic acid (CBGA)	1.23
Cannabidiol (CBD)	9.34
Tetrahydrocannabivarin (THCV)	nd
Delta-9-tetrahydrocannabinol (THC)	nd
Cannabichromene (CBC)	nd
Tetrahydrocannabinolic acid (THCA)	nd
Cannabichromenic acid (CBCA)	nd
Cannabielsoin (CBE)	0.04
Saturated fat	9.3
ω-9 fatty acids	8.6
ω-3 fatty acids	21.1
ω-6 fatty acids	59.9

Table 2
Concentrations of cannabidiol (CBD) and cannabidiolic acid (CBDA) in HOE over time. Data are expressed as mean ± RSD of 4 serial dilutions, each dilution run in triplicates.

Experiments	CBD %, g/g	CBDA %, g/g
1.	2.98 ± 1.13	0.59 ± 0.64
2.	2.97 ± 1.92	0.59 ± 1.40
3.	3.33 ± 0.84	0.56 ± 2.93

2.4. Chronic constriction injury (CCI)

We elicited peripheral neuropathy in the left sciatic nerve of mice as described elsewhere [4]. In brief, mice were anesthetized in 2–3% isoflurane in O_2. Under aseptic conditions, the sciatic nerve was exposed at mid-thigh level through a small incision and loosely tied at 3 distinct sites (spaced at 1-mm interval) with 4–0 chromic catgut (Ethicon, USA). The wound was closed with a single muscle suture (Mersilk 5.0, Ethicon, USA) and glue to fasten the skin. Operated mice were returned to their home cages for recovery. Test compounds or vehicle were given by the oral route on day 7 after surgery (acute treatment) and then repeatedly once daily for 7 consecutive days (subchronic treatment). Behavioral tests were performed within 1 h of acute treatment or last subchronic treatment in both operated (ipsilateral) and contralateral paws. Mice were sacrificed by decapitation, the spinal cords were extruded by hydraulic pressure and processed for specific mRNA quantification in lumbar segments by real-time quantitative PCR.

2.5. Behavioral testing

Mechanical sensitivity was assessed using a dynamic plantar aesthesiometer (Cat. N° 37450, Ugo Basile, Italy). Mice were placed individually in transparent cages positioned on a wire mesh surface. After a 45-min habituation period, a mechanical stimulus was delivered to the plantar surface of the hind paws through the metal grid by an automated steel filament exerting an increasing force ranging from 0 to 5 g over 10 s. The force at which the mouse withdrawn its paw (withdrawal

threshold, in grams) was measured automatically. Thermal sensitivity was measured using a Hargreaves plantar test apparatus (San Diego Instruments, Inc, CA, USA). Mice were individually placed in small enclosures with a glass floor. After a 45-min habituation period, the plantar surface of the hind paws was exposed to a beam of radiant heat (infrared heat intensity: 3.0) through the glass floor. The cut-off time was set at 15 s. The time taken to withdraw the paw from heat stimulus (withdrawal latency, in seconds) was measured automatically. Each paw was tested 3 times with a 2-min interval between stimuli and the mean paw withdrawal threshold and latency were calculated. Paw thickness was measured in both ipsilateral and contralateral paws using a digital caliper (Cat. N° 06–664–16, Fisher scientific, USA). Paw edema was quantified as the difference (Δpaw thickness, in mm) between the ipsilateral paw thickness and the contralateral counterpart.

2.6. Real-time quantitative PCR

We extracted total RNA from lumbar spinal cords (L3-L6) using TRIzol™ reagent (Thermo Fisher Scientific, Walthman, USA) and purified with the PureLink™ RNA Mini Kit (Invitrogen, Carlsbad, USA) as directed by the supplier. Prior to purification, samples were rendered genomic DNA-free by passing the isolated RNA extract through a gDNA Eliminator spin column (Qiagen, Germantown, USA). RNA concentration and purity were determined using the NanoDrop 2000/2000-c spectrophotometer (Thermo Fisher Scientific, Walthman, USA). cDNA was synthesized using 2 μg of total RNA as input for the High-Capacity cDNA RT Kit with RNase Inhibitor (Applied BioSystems, Foster City, USA) with a final reaction volume of 20 μL. First-strand cDNA was amplified using TaqMan™ Universal PCR Master Mix (Thermo Fisher Scientific, Walthman, USA) following the manufacturer's instructions. Real-time PCR primers and fluorogenic probes were purchased from Applied Biosystems (TaqMan(R) Gene Expression Assays, Foster City, CA). We used TaqMan gene expression assays for mouse Actin-β (Mm00607939_s1), *Hprt* (Mm00446968_m1), *Gapdh* (Mm99999915_g1), *Tnf-α* (Mm00443258_m1), *Il-1β* (Mm00434228_m1), *Il-6* (Mm00446190_m1), and *Il-10* (Mm00439614_m1) (Applied Biosystems, Foster City, CA). Real-time PCR reactions were performed in 96-well plates using CFX96™ Real-Time System (Bio-Rad, USA). The thermal cycling conditions were as follows: initial denaturation set at 95 °C for 10 min, followed by 45 cycles, where each cycle was performed at 95 °C for 30 s and at 55 °C for 60 s. The Bestkeeper software was used to determine the expression stability and the geometric mean of three different housekeeping genes (*Actb*, *Hprt* and *Gapdh*). ΔCt values were calculated as the difference between the Ct value of the geometric mean of these housekeeping genes and the Ct value of the genes of interest. The relative quantity of genes of interest was calculated by the $2^{-\Delta\Delta Ct}$ method and expressed as fold change over vehicle control.

2.7. Pharmacokinetic experiments

We administered HOE (100 mg-kg^{-1}), PEA (10 or 20 mg-kg^{-1}) or the combinations of both to adult mice in volumes of 10 mL-kg^{-1} by the oral route. The animals were deeply anesthetized with isoflurane at various time points following test compounds administration (0, 15, 30, 45 and 60 min), blood was collected by cardiac puncture into ethylenediaminetetraacetic acid (EDTA)-rinsed syringes and transferred into 1 mL polypropylene plastic tubes containing spray-coated potassium-EDTA (K_2-EDTA). Plasma was prepared by centrifugation at 1450 × *g* at 4 °C for 15 min, and transferred into polypropylene tubes, which were immediately frozen and stored at −80 °C. Animals were euthanized by decapitation, their spinal cords were quickly extruded by hydraulic pressure on an ice-cold glass plate and lumbar segments were harvested, frozen on dry ice and stored −80 °C until analyses.

2.8. Sample preparation

2.8.1. Extraction of PEA, anandamide (AEA) and 2-arachidonoyl-sn-glycerol (2-AG)

Extraction method was described elsewhere [2,22]. Plasma (50 μL) was transferred into 8-mL glass vials and diluted with water (0.9 mL) and 50 μL of the following internal standards (ISTD): [$^2H_4$]-PEA, [$^2H_4$]-AEA, and [$^2H_5$]−2-AG (100 nM each). Samples were loaded onto preconditioned Oasis HLB cartridges (Waters Corporation, Milford Massachusetts, USA) washed with methanol (100%) and water and eluted under vacuum (3–5 mmHg). The cartridges were rinsed with methanol (40%). Acetonitrile (1 mL) was added, and vacuum pressure was increased gradually to 10 mmHg to ensure maximal analyte recovery. Eluates were dried under nitrogen and reconstituted in 100 μL of acetonitrile. Samples were transferred to deactivated glass inserts (200 μL) and placed inside amber glass vials (2 mL; Agilent Technologies, Wilmington, DE). Lumbar spinal cords (~15 mg) were transferred into 2 mL Precellys soft tissue tubes (Bertin Instruments, France) and spiked with 50 μL of ISTD ([$^2H_4$]-PEA, [$^2H_4$]-AEA, and [$^2H_5$]−2-AG,100 nM each) and ice-cold acetone (1 mL). Samples were homogenized at 4 °C, 6000 rpm, 15 s/cycle for 2 cycles with 20 s pause in between. The supernatants were carefully transferred into 8-mL glass vials and dried under nitrogen. 3 mL of chloroform/methanol (2:1, v/v) and 1 mL of water were added to the samples, which were then stirred vigorously and centrifuged at 3000 rpm for 15 min at 4 °C. The lower phases were collected, while upper phases were extracted again with chloroform (2 mL). Eluates were dried under nitrogen and reconstituted in 100 μL of acetonitrile. Samples were transferred to deactivated glass inserts (200 μL) and placed inside amber glass vials (2 mL).

2.8.2. CBD and CBDA extraction

Extraction method was described previously [45]. We weighed HOE (8–10 mg) in 8-mL glass vials, added 5 mL of ethanol and stirred vigorously. The samples were diluted 100-fold with methanol and the diluted solutions (0.5 mL) were spiked with 5 μL of [$^2H_3$]-CBD (5.0 μg/mL) and filtered through a 0.45 μm syringe filter (Agilent Technologies, Wilmington, DE) followed by serial dilutions in methanol directly into 200 μL glass inserts placed in 2.0 mL vials. Plasma (100 μL) was transferred into 8-mL glass vials and mixed with 50 μL of [$^2H_3$]-CBD (100 ng/mL). Proteins were precipitated by addition of 0.5 mL ice-cold acetonitrile containing 1% formic acid. Lumbar spinal cord samples (~15 mg) were transferred into 2 mL Precellys soft tissue tubes and spiked with 50 μL of [$^2H_3$]-CBD (100 ng/mL) and 1 mL of ice-cold acetonitrile containing 1% formic acid. Spinal cord samples were then homogenized as described above, and the supernatants were carefully transferred into 8-mL glass vials. Plasma and spinal cord supernatants were stirred vigorously and centrifuged at 3000 rpm for 15 min at 4 °C. After centrifugation, the supernatants were loaded onto 1 mL Captiva EMR lipid cartridges (Agilent Technologies, USA) and eluted under vacuum (3–5 mmHg). Tissue pellets were rinsed with water/acetonitrile (1:4, v/v; 0.2 mL), stirred for 30 s, and centrifuged at 3000 rpm for 15 min at 4 °C. The supernatants were collected, transferred onto EMR cartridges, eluted, and pooled with the first eluate. The cartridges were rinsed with water/acetonitrile (1:4, v/v; 0.2 mL). Eluates were dried under a nitrogen and reconstituted in 100 μL of methanol containing 0.1% formic acid. Samples were transferred to deactivated glass inserts (200 μL) and placed inside amber glass vials (2 mL).

2.9. Liquid chromatography/tandem mass spectrometry (LC-MS/MS) analysis

LC separations were carried out using a 1260 series LC system (Agilent Technologies, Santa Clara, CA), consisting of a binary pump with degasser, thermostated autosampler and column compartment coupled to a 6460 C triple-quadrupole mass spectrometric detector (MSD; Agilent Technologies, Santa Clara, CA). Analytes were separated

on an Eclipse XDB C18 column (1.8 μm, 2.1 × 30.0 or 50.0 mm; Agilent Technologies, Wilmington, DE). For CBD and CBDA analyses, the mobile phase consisted of water containing 0.1% formic acid as solvent A and methanol containing 0.1% formic acid as solvent B [45]. Representative LC-MS/MS tracings are illustrated in Supplementary Fig. 1–3. For PEA, AEA and 2-AG analyses, the mobile phase consisted of water containing 0.25% acetic acid and 5 mM ammonium acetate as solvent A and methanol containing 0.25% acetic acid and 5 mM ammonium acetate as solvent B [2]. The flow rate was 0.3–0.5 mL/min. The step-gradient conditions were as follows. CBD and CBDA: starting at 72% B for 1.50 min, changed to 95% B at 1.51 min, and maintained till 2.5 min to remove any strongly retained materials from the column; the column was re-equilibrated for 3.5–5 min to 72% B before the next injection. PEA, AEA and 2-AG: starting at 78% B to 28% B in 8.00 min, changed to 95% B at 8.01 min, and maintained till 10.00 min; then changed back to 78% B at 10.01 min; the equilibration time was 5 min. The column temperature was maintained at 40 °C and the autosampler at 9 °C. The total analysis time, including re-equilibration, was 6.0–15.0 min. The injection volume was 2.0 μL. To prevent carry over, the needle was washed in the autosampler port for 30 s before each injection, using a wash solution consisting of 10% acetone in water/-methanol/isopropanol/acetonitrile (1:1:1:1, v/v). The MSD was operated in the positive electrospray ionization (ESI) mode, and analytes were quantified by multiple reaction monitoring (MRM), the acquisition parameters are given in Supplementary Table 1. The capillary and nozzle voltages were 3500 V and 300–500 V, respectively. The drying gas temperature was 300–350 °C with a flow of 9.0–11.0 L/min. Sheath gas temperature was 300–375 °C with a flow of 12 L/min. Nebulizer pressure was set at 45–50 psi. The MassHunter software (Agilent Technologies, Santa Clara, CA) was used for instrument control, data acquisition and analysis.

2.10. Statistical analysis

Results are presented as mean ± S.E.M. of n experiments. ED_{50} values were determined by linear regression analysis of dose-response curves. Individual slopes of the dose-response curves were compared by Student's *t*-test, according to the test of parallelism. Analyses were conducted using Prism software (GraphPad Software, San Diego, CA, Version 8.4.2). Areas under the time-course curves (AUC) were calculated using the trapezoidal rule. Differences between groups were determined by one- or two-way analysis of variance (ANOVA) followed by Dunnett's test for multiple comparisons, as appropriate. The significance level was set at $P < 0.05$.

3. Results

3.1. Antinociceptive effects of HOE

To assess the antinociceptive effects of HOE, we first used the formalin test as a model of injury-induced spontaneous pain [13]. A single dose of the extract (10, 50 and 100 mg-kg^{-1}) was given orally to male mice 1 h before intraplantar injection of formalin. As expected [13], the chemical irritant produced an immediate nocifensive response consisting of two temporally distinct phases of licking and flinching of the injected limb (Fig. 1, A and B; phase I: 0–10 min; phase II: 15–60

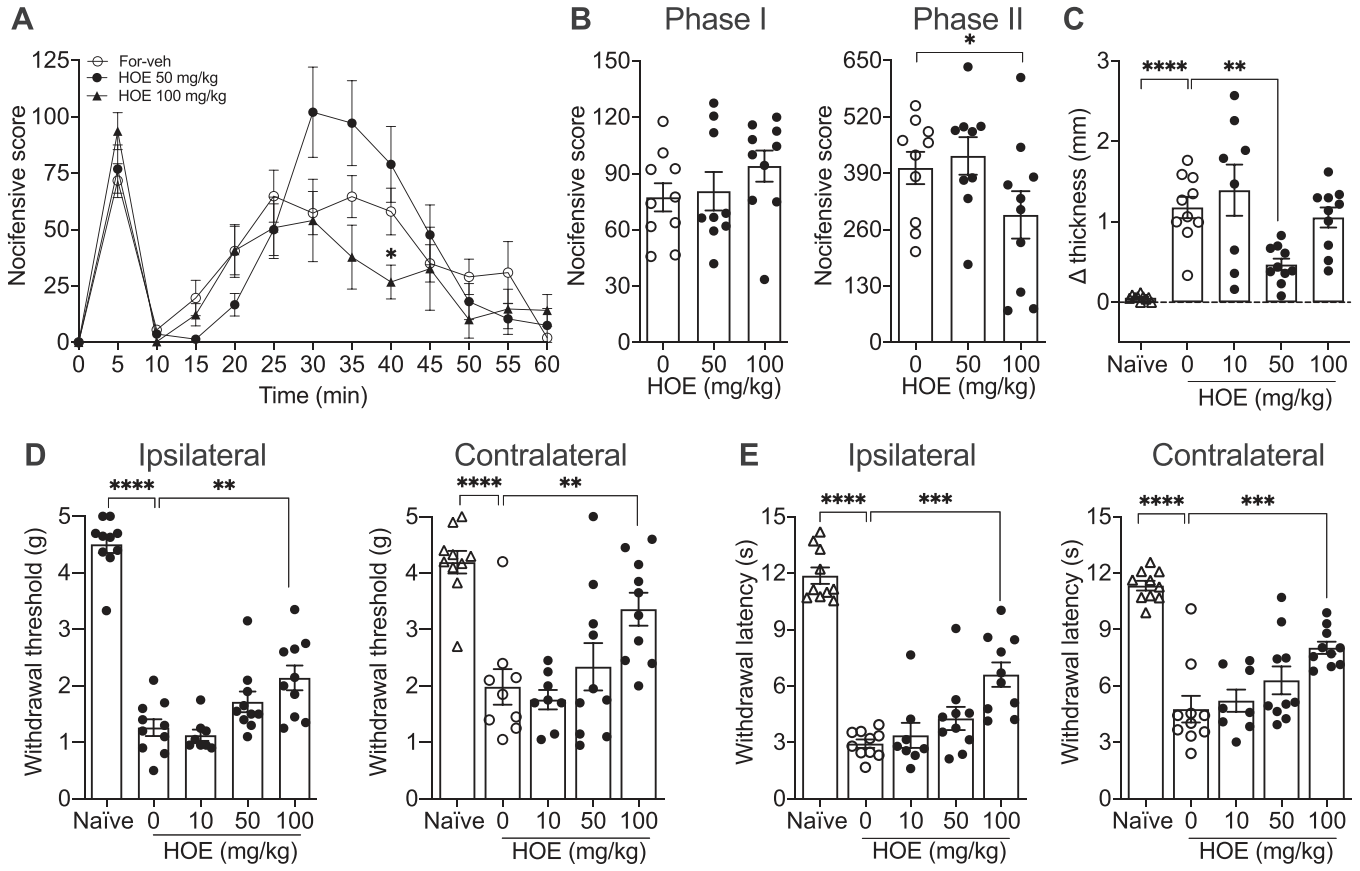

Fig. 1. Effects of a single dose of HOE on formalin-evoked acute and persistent nociceptive behaviors. (A) Time-course of the acute nocifensive response to formalin (1%, v/v). (B) Cumulative score of the phase I and phase II of the acute nocifensive response. (C) Paw thickness (injected paw thickness minus non-injected, in mm) at PFD7. (D) Formalin-evoked mechanical allodynia and (E) heat hyperalgesia to both ipsilateral and contralateral paws at PDF7. Data are expressed as mean ± S.E.M (n = 8–10 per group) and analyzed by two-way (A and B) or one-way (C, D and E) ANOVA followed by Dunnett's test for multiple comparisons. *$P < 0.05$, **$P < 0.01$, ***$P < 0.001$ and ****$P < 0.0001$ vs. Sham or Vehicle controls.

min). On post formalin day (PFD) 7, the acute pain event gave way to edema in the injected paw (Fig. 1, C) and hypersensitivity in both ipsilateral and contralateral paws (Fig. 1, D and E).

The results show that HOE (100 mg-kg^{-1}) administration had no effect on the nocifensive score in Phase I, but reduced Phase II behavior by 27% ($P < 0.05$ vs. vehicle) (Fig. 1, A–B). On PDF7, mechanical allodynia was also attenuated by 27% ($P < 0.01$ vs. vehicle) and 62% ($P < 0.01$ vs. vehicle), respectively, in ipsilateral and contralateral paws of mice that had received HOE (100 mg-kg^{-1}) (Fig. 1, D). Heat hyperalgesia was alleviated by 41% ($P < 0.001$ vs. vehicle) and 50% ($P < 0.001$ vs. vehicle) in ipsilateral and contralateral paws, respectively (Fig. 1, E). Moreover, HOE reduced paw edema by 63% at 50 mg-kg^{-1} ($P < 0.01$ vs. vehicle) but had no such effect at 100 mg-kg^{-1} ($P > 0.05$ vs. vehicle) (Fig. 1, C).

Next, we produced peripheral neuropathy in mice by ligating their right sciatic nerve, which resulted in the development of mechanical allodynia and heat hyperalgesia in the operated limb (Fig. 2). On day 7 after surgery, we administered HOE by the oral route 1 h before testing. The results show that administration of a single dose of HOE (100 mg-kg^{-1}) had no effect on either heat hyperalgesia or mechanical allodynia (Fig. 2, A and B; $P > 0.05$ vs. vehicle), whereas a 7-day treatment with the extract (100 mg-kg^{-1}) decreased heat hyperalgesia by 33% (Fig. 2, C and D; $P < 0.01$ vs vehicle).

3.2. Antinociceptive effects of PEA

As expected from previous work [6,24], administration of PEA (10, 30, 100 and 300 mg-kg^{-1}, oral) resulted in a dose-dependent suppression of formalin-evoked nocifensive (Fig. 3, A–B) and inflammatory (Fig. 3C) responses. Mechanical allodynia on PFD7 was also attenuated by 91% ($P < 0.0001$ vs. vehicle) and 112% ($P < 0.0001$ vs. vehicle), respectively in ipsilateral and contralateral paws of mice that had received the highest dose of PEA (300 mg-kg^{-1}) (Fig. 3, D). A similar effect was seen with heat hyperalgesia, which was alleviated by 93% ($P < 0.0001$ vs. vehicle) and 110% ($P < 0.0001$ vs. vehicle) in ipsilateral and contralateral paws, respectively (Fig. 3, E). At dosages lower than 300 mg-kg^{-1}, PEA had no effect on either mechanical allodynia or heat hyperalgesia ($P > 0.05$ vs. vehicle).

In the CCI model, a single PEA administration produced strong dose-dependent suppression of mechanical allodynia (ED_{50} = 22.2 mg-kg^{-1}; 95% confidence interval [CI] ranging from 18.7 to 26.0 mg-kg^{-1}; Fig. 4, A and B) and heat hyperalgesia (ED_{50} = 25.1 mg-kg^{-1}; 95% CI ranging from 21.8 to 29.1 mg-kg^{-1}; Fig. 4, D and E) by up to 85% ($P < 0.0001$ vs. vehicle) and 109% ($P < 0.0001$ vs. vehicle), respectively.

The two highest doses of PEA (100 or 300 mg-kg^{-1}) were administered orally to neuropathic mice once daily for 7 consecutive days. The treatment reversed mechanical allodynia (Fig. 4, C) and heat hyperalgesia (Fig. 4, F), supporting prior studies indicating that there is no tolerance to the antinociceptive effects of PEA [24].

3.3. Antinociceptive effects of combinations of HOE and PEA

Next, we tested whether HOE and PEA might interact when given in combination. Our results did not allow us to determine a median effective dose for HOE in either of the two experimental pain models, which made it impossible to evaluate the pharmacodynamic interactions between PEA and HOE by isobolographic analysis. Instead, we opted for a combination subthresholding approach which is a valid, effect-based strategy to investigate the biological activity of combinations of two or more compounds [14]. We administered combinations of sub-effective oral doses of HOE (50 mg-kg^{-1}) and PEA (30 or 100 mg-kg^{-1}) 1 h before formalin (1% v/v). The results show that the HOE (50 mg-kg^{-1}) and PEA (30 mg-kg^{-1}) combination did not affect Phase I of formalin-evoked nocifensive behavior but reduced Phase II by 32% ($P < 0.01$ vs. vehicle) (Fig. 5, A and B). There was no effect on paw edema (Fig. 5, C).

On PFD7, formalin-evoked mechanical allodynia was attenuated by 49% ($P < 0.0001$ vs. vehicle) and 75% ($P < 0.0001$ vs. vehicle) respectively, in the ipsilateral and contralateral paws of mice that had received HOE (50 mg-kg^{-1}) plus PEA (100 mg.kg^{-1}) (Fig. 5, D). Likewise, heat hyperalgesia was decreased by 54% ($P < 0.0001$ vs. vehicle) and 57% ($P < 0.0001$ vs. vehicle), respectively, in the ipsilateral and contralateral paws (Fig. 5, E).

Finally, we asked whether the combination of HOE and PEA might affect hypersensitivity in the CCI model. We administered combinations of sub-effective oral doses of HOE (100 mg-kg^{-1}) and PEA (10 or 20 mg-kg^{-1}). Fig. 6 shows that the combinations reduced mechanical allodynia (Fig. 6, A) and heat hyperalgesia (Fig. 6, B) in the operated limbs by as much as 85% ($P < 0.001$ vs. vehicle) and 118% ($P < 0.001$ vs. vehicle), respectively.

3.4. RT-qPCR measurements

We examined whether HOE (100 mg-kg^{-1}), PEA (20 mg-kg^{-1}) or their

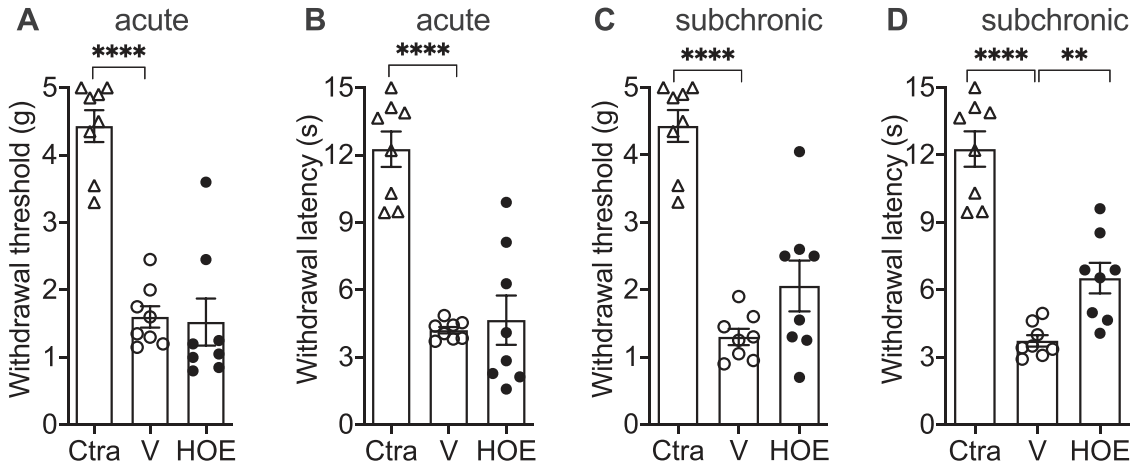

Fig. 2. Effects of HOE on CCI-evoked mechanical allodynia (A and C) and heat hyperalgesia (B and D). A single dose of HOE (100 mg.kg-1) was administered orally to neuropathic mice on day 7 after CCI surgery (acute) and then repeatedly for 7 consecutive days (subchronic). (A and B) Mechanical allodynia and heat hyperalgesia on day 7 after CCI surgery. (C and D) Mechanical allodynia and heat hyperalgesia on day 14 after CCI surgery. Data are expressed as mean ± S.E.M (n = 8 per group) and analyzed by oneway ANOVA followed by Dunnett's test for multiple comparisons. **$P < 0.01$ vs. Vehicle (V) and ****$P < 0.0001$ vs. Contralateral (Ctra; from vehicle-treated mice) controls.

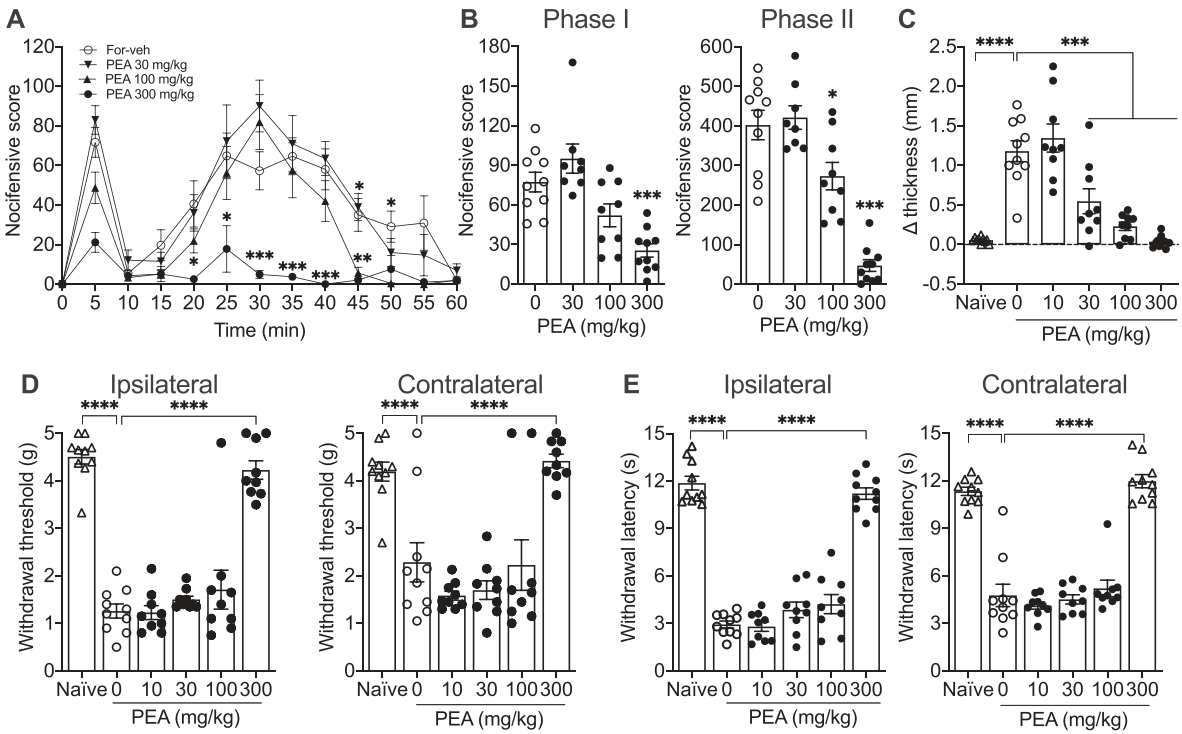

Fig. 3. Effects of a single dose of PEA on formalin-evoked acute and persistent nociceptive behaviors. (A) Time-course of the acute nocifensive response to 1% formalin. (B) Cumulative score of the phase I and phase II of the acute nocifensive response. (C) Paw thickness (injected paw thickness minus non injected, in mm) at PFD7. (D) Mechanical and (E) heat sensitivities to both ipsilateral and contralateral paws at PDF7. Data are expressed as mean ± S.E.M (n = 8–12 per group) and analyzed by two-way (A and B) or one-way ANOVA (C, D and E) followed by Dunnett's test for multiple comparisons. *$P < 0.05$, **$P < 0.01$, ***$P < 0.001$ and ****$P < 0.0001$ vs. Sham or Vehicle controls.

combination might alter the transcription of proalgesic and inflammatory cytokines in lumbar spinal cords. The results show that CCI was associated with statistically detectable increases in IL-6 and IL-10 mRNA expression (Fig. 7, A and B). IL-6 increased 2 folds ($P < 0.05$ vs. sham) while IL-10 increased 2.5 folds ($P < 0.01$ vs. sham). IL-1β mRNA levels were also increased but this trend failed to reach statistical significance (Fig. 7, C). By contrast, there were no statistically detectable changes in the expression of TNF-α mRNA (Fig. 7, D). Oral administration of a single dose of HOE (100 mg-kg^{-1}) to neuropathic mice normalized IL-6 ($P < 0.01$ vs. vehicle) and IL-10 ($P < 0.01$ vs. vehicle) mRNA levels (Fig. 7, A and B). When administered alone, PEA (20 mg-kg^{-1}) halved IL-10 mRNA levels ($P < 0.05$ vs. vehicle). The combination of HOE (100 mg-kg^{-1}) and PEA (20 mg-kg^{-1}) caused a 1.7-fold decrease in IL-6 mRNA expression ($P < 0.05$ vs. vehicle), while lowering IL-10 mRNA levels 3.7 folds ($P < 0.001$ vs. vehicle).

3.5. Pharmacokinetic profiles of HOE, PEA or their combination

We measured the concentrations of PEA, CBD and CBDA in mouse plasma (Fig. 8) and spinal cord tissue (Fig. 9) in a 60-min period following oral administration of a single dose of the compounds or their combination. Fig. 8 shows concentration-time curves and overall exposure (area-under-the-curve, AUC) to PEA (A), CBD (B) and CBDA (C). Baseline levels of PEA were 10.03 ± 0.4 pmol-mL^{-1}. Oral administration of HOE did not affect baseline PEA concentrations (Fig. 8, A). By contrast, plasma PEA levels increased rapidly by up to 44.1 ± 2.4 pmol-mL^{-1} ($P < 0.01$ vs. baseline) and 66.9 ± 4.9 pmol-mL^{-1} ($P < 0.05$ vs. baseline) after administration of PEA or the combination of HOE with PEA, respectively. Importantly, the combination of HOE with PEA (AUC = 2211 ± 208 pmol-min-mL^{-1}) resulted in greater exposure to PEA than HOE (AUC = 72.1 ± 83.9 pmol-min-mL^{-1}; $P < 0.0001$ vs HOE + PEA) and PEA (AUC = 1516 ± 133.2 pmol-min-mL^{-1}; $P < 0.05$ vs HOE + PEA) given separately, suggesting that HOE enhances the bioavailability of PEA and prolongs its lifetime in circulation.

To assess whether PEA might affect the pharmacokinetic profile of HOE, we administered HOE, either alone or in combination with PEA, and measured plasma concentrations of two main components of HOE, CBD and CBDA. The results show that plasma CBD levels increased rapidly to 1676 ± 289.6 pmol-mL^{-1} ($P < 0.05$ vs. baseline) and 1826 ± 635.6 pmol-mL^{-1} ($P < 0.05$ vs. baseline) after administration of HOE or the combination of HOE with PEA, respectively (Fig. 8, B). Likewise, CBDA increased up to 39,917 ± 2042 pmol-mL^{-1} and 38,971 ± 5289 pmol-mL^{-1} after administration of HOE or the combination of HOE with PEA, respectively (Fig. 8, C). However, the combination of HOE with PEA [AUC (CBD) = 52,153 ± 13,999 pmol-min-mL^{-1}; AUC (CBDA) = 142,1014 ± 162,688 pmol-min-mL^{-1}] did not alter the overall exposure to CBD (Fig. 8, B) and CBDA (Fig. 8, C) compared to HOE alone [AUC (CBD) = 56,334 ± 7757 pmol-min-mL^{-1}; AUC (CBDA) = 14,15702 ± 70,988 pmol-min-mL^{-1}], suggesting that PEA does not alter the pharmacokinetic properties of HOE.

Fig. 9 shows concentration-time curves and overall exposure to PEA (A), CBD (B) and CBDA (C) in mouse lumbar spinal cords. Baseline levels of PEA were 117.1 ± 6.3 pmol-mg^{-1} of tissue (Fig. 9, A). Oral administration of HOE, PEA or their combination had no statistically detectable effect on such levels in the 60-min time frame of this study. This finding suggests that PEA does not readily enter the spinal cord and may exhibit its analgesic action mainly through a peripheral mechanism [6]. By contrast, we were able to detect appreciable amounts of CBD and CBDA in spinal cord after oral administration of HOE alone or in combination with PEA (Fig. 9, B–C). Of note, oral administration of the combination of HOE with PEA [AUC (CBD) = 29.21 ± 7.36 pmol-min-mg^{-1}; AUC (CBDA) = 43.28 ± 13.64 pmol-min-mg^{-1}] did not statistically change the overall exposure of mice to CBD and CBDA compared with HOE alone [AUC (CBD) = 36.3 ± 5.78 pmol-min-mg^{-1}; AUC (CBDA) = 59.04 ± 17.48 pmol-min-mg^{-1}], suggesting that PEA does not affect the distribution of hemp in the spinal cord.

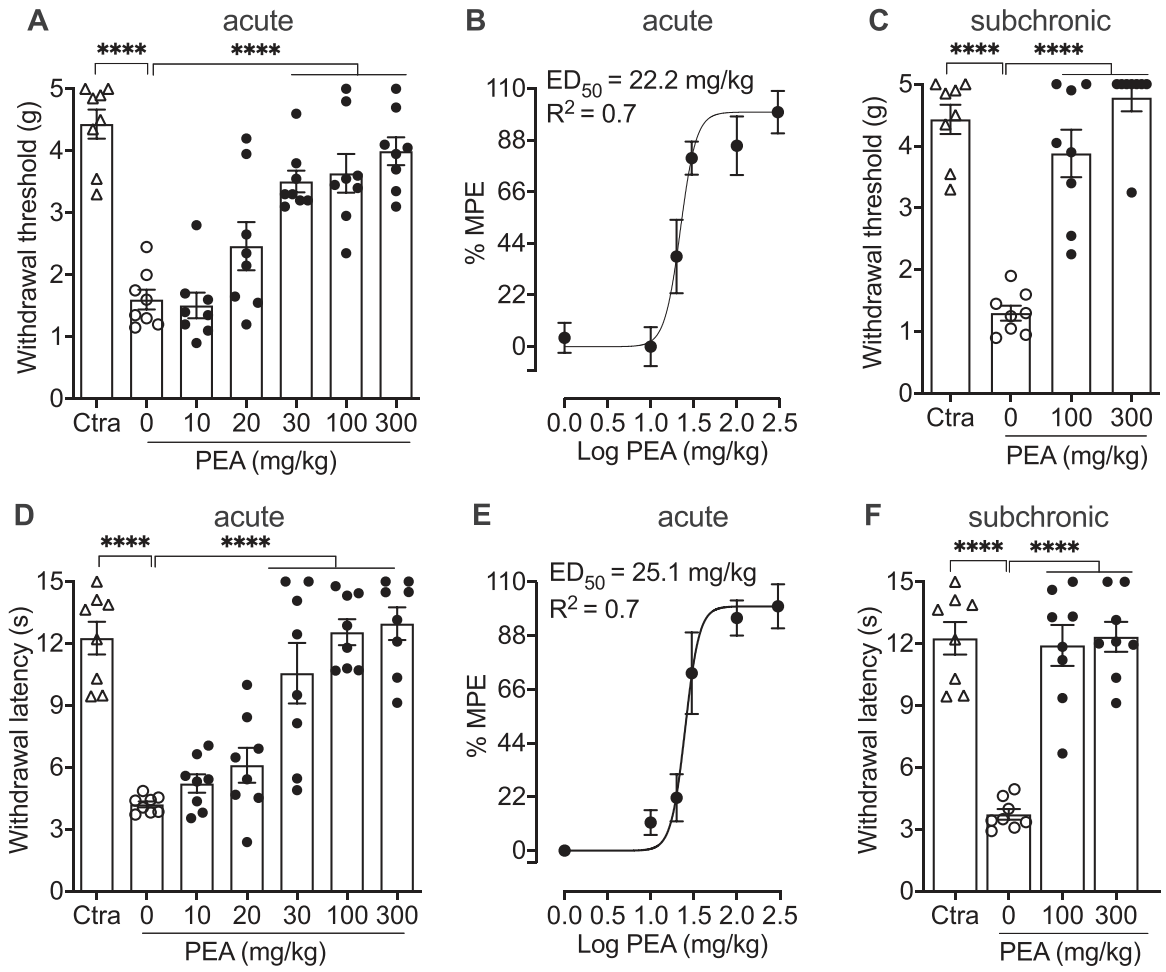

Fig. 4. Effects of PEA on CCI-evoked mechanical allodynia (A-C) and heat hyperalgesia (D-F). PEA was administered orally to neuropathic mice on day 7 after CCI surgery (acute) and then repeatedly for 7 consecutive days (subchronic). Dose-response curves for the effects of PEA on CCI-induced mechanical allodynia (A, B) and heat hyperalgesia (D, E) on day 7 after surgery. Effects of subchronic administration of PEA (100 and 300 mg.kg-1) on CCI-induced mechanical allodynia (C) and heat hyperalgesia (F) on day 14 after surgery. Data are expressed as mean ± S.E.M (n = 8 per group) and analyzed by one-way ANOVA followed by Dunnett's test for multiple comparisons. $^{**}P < 0.01$ vs. Vehicle (V) and $^{****}P < 0.0001$ vs. Contralateral (Ctra) controls. %MPE, % maximal possible effect.

3.6. Effects of HOE alone or in combination with PEA on endocannabinoid levels

We measured the concentrations of the endocannabinoids AEA and 2-AG in mouse plasma and spinal cord tissue after oral administration of a single dose of HOE (100 mg-kg^{-1}) alone or in combination with PEA (20 mg-kg^{-1}). Fig. 10 shows that HOE alone or in combination with PEA did not affect plasma (Fig. 10, A and B) or spinal cord (Fig. 10, C and D) levels of the compounds ($P > 0.05$ vs baseline) in the 60-min time frame of this study. These findings suggest that acute administration of HOE alone or in combination with PEA does not affect the endocannabinoid levels in mice.

4. Discussion

Legislative changes have increased the availability of products derived from industrial hemp (i.e., cannabis containing < 0.3% Δ^9-THC), which are now widely used for self-medication of pain and other medical conditions [7]. Still very little is known, however, about the pharmacological properties of such products. In the present study, we set out to assess the efficacy of a full spectrum HOE, alone or in combination with PEA, in two complementary mouse models of pain, the formalin and CCI tests. We found that HOE has little or no effect when administered alone but synergizes with PEA to produce a greater-than-additive alleviation of pain-related behaviors. Pharmacokinetic studies suggest that one possible explanation for this synergistic interaction lies in the ability of HOE to prolong the exposure and lifetime of PEA in circulation.

Hemp contains a wide range of phytocannabinoids, terpenes, flavonoids and other bioactive molecules which likely contribute to its biological effects both individually and synergistically [36]. Identifying which of these myriad chemicals might be responsible for the modest antinociceptive properties of HOE would be a daunting task, but promising candidates include, among others, CBD and CBDA. For example, it has been shown that CBD produces antinociceptive effects in some animal models without causing apparent tolerance [18,20,26,47,49,5,8,9]. Likewise, studies have shown that CBDA exhibits antinociceptive and anti-inflammatory properties in rodents [35,50].

Cellular components of the immune system are thought to contribute to pain initiation and maintenance through the release of multiple cytokines [34,40,43]. The present results show that mRNA levels of IL-6 and IL-10 increased significantly in lumbar spinal cord tissue on day 7 after CCI surgery, an effect that was reduced by HOE alone or by the HOE/PEA combination. The increase in spinal IL-6 and IL-10 transcription is consistent with previous reports [12,15,3,39]. The finding that CCI had little to no impact on IL-1β and TNF-α mRNAs is also in line with prior studies [10,39,41]. Oral administration of HOE either alone, or in combination with PEA caused a reduction in the mRNA expression

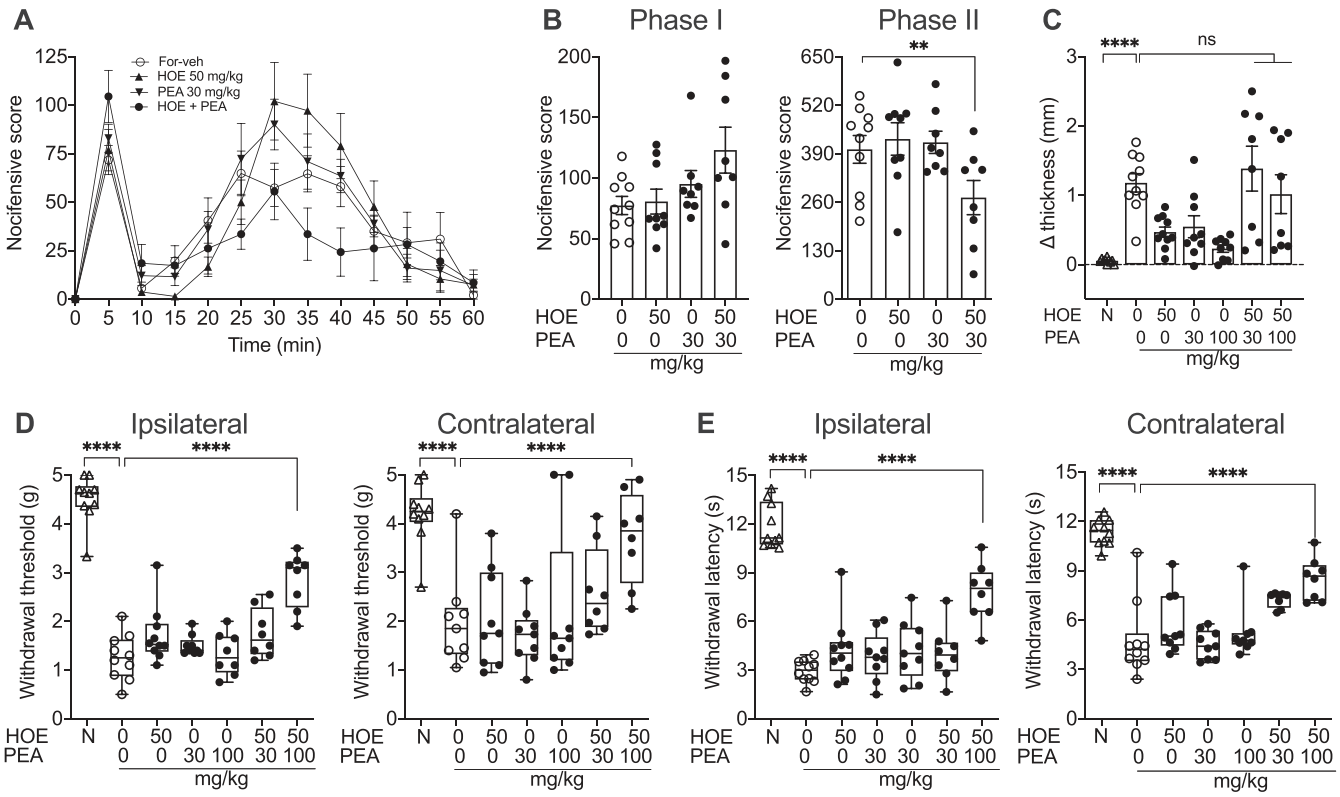

Fig. 5. Effects of combinations of HOE with PEA on formalin-evoked acute and persistent nociceptive behaviors. (A) Time-course of the acute nocifensive response to 1% formalin. (B) Cumulative score of the phase I and phase II of the acute nocifensive response. (C) Paw thickness (injected paw thickness minus non injected, in mm) at PFD7. (D) Mechanical and (E) heat sensitivities to both ipsilateral and contralateral paws at PDF7. Data are expressed as mean ± S.E.M (n = 8–10 per group) and analyzed by two-way (A and B) or one-way ANOVA followed by Dunnett's (C, D and E) test for multiple comparisons. *$P < 0.05$, **$P < 0.01$, ***$P < 0.001$ and ****$P < 0.0001$. N: naïve; ns: nonsignificant.

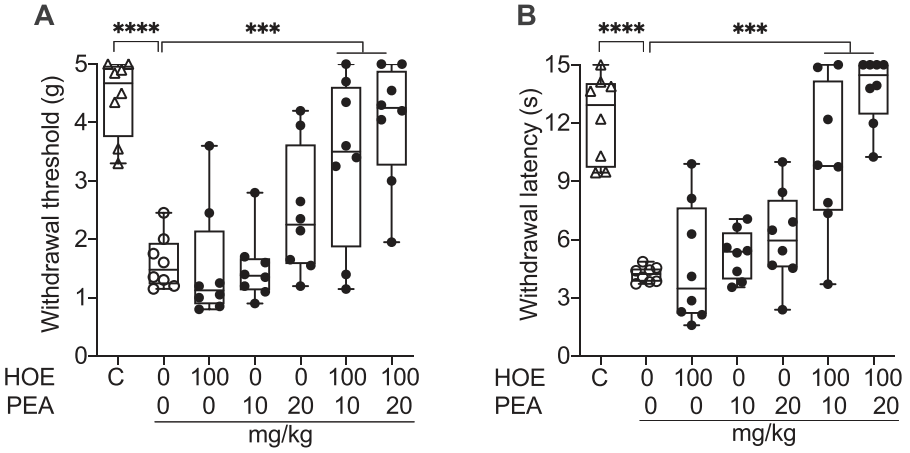

Fig. 6. Effects of combinations of HOE with PEA on CCI-evoked mechanical allodynia (A) and heat hyperalgesia (B) to operated limbs. A single dose of HOE (100 mg.kg-1), alone or in combination with PEA (10 mg.kg-1) or PEA (20 mg.kg-1) was administered orally to neuropathic mice 1 h before testing. Data are expressed as mean ± S.E.M. (n = 8 per group) and analyzed by one-way ANOVA followed by Dunnett's test for multiple comparisons. * $P < 0.05$, **$P < 0.01$, ***$P < 0.001$ and ****$P < 0.0001$. C, contralateral.

of IL-6 and IL-10. This finding is relevant from a therapeutic perspective as the inhibition of IL-6 with neutralizing antibodies or other pharmacological tools has been found to alleviate nociceptive behaviors suggestive of neuropathic pain [1,28].

An important finding of the present report is that one or more chemical constituents of hemp interact(s) with the endogenous analgesic and anti-inflammatory compound PEA to produce greater-than-additive antinociceptive effects. This synergism may be underpinned by pharmacodynamic and/or pharmacokinetic mechanisms. An antinociceptive synergism has been previously demonstrated between PEA and the endocannabinoid anandamide, which act via PPAR-α and CB_1 cannabinoid receptors, respectively [38]. This mechanism is unlikely to be operational in our studies, however, because we found no evidence for enhanced endocannabinoid signaling after administration of the HOE/PEA combination, at least in plasma and spinal cord tissue at the time of measurement. While other pharmacodynamic interactions might have occurred, our results point to the possibility that the synergistic potentiation between HOE and PEA could have a pharmacokinetic underpinning. Indeed, we found that administering a combination of HOE and PEA enhances and prolongs the systemic exposure to PEA, compared to administering PEA alone. By contrast, PEA did not affect the pharmacokinetic properties of two quantitatively major constituents

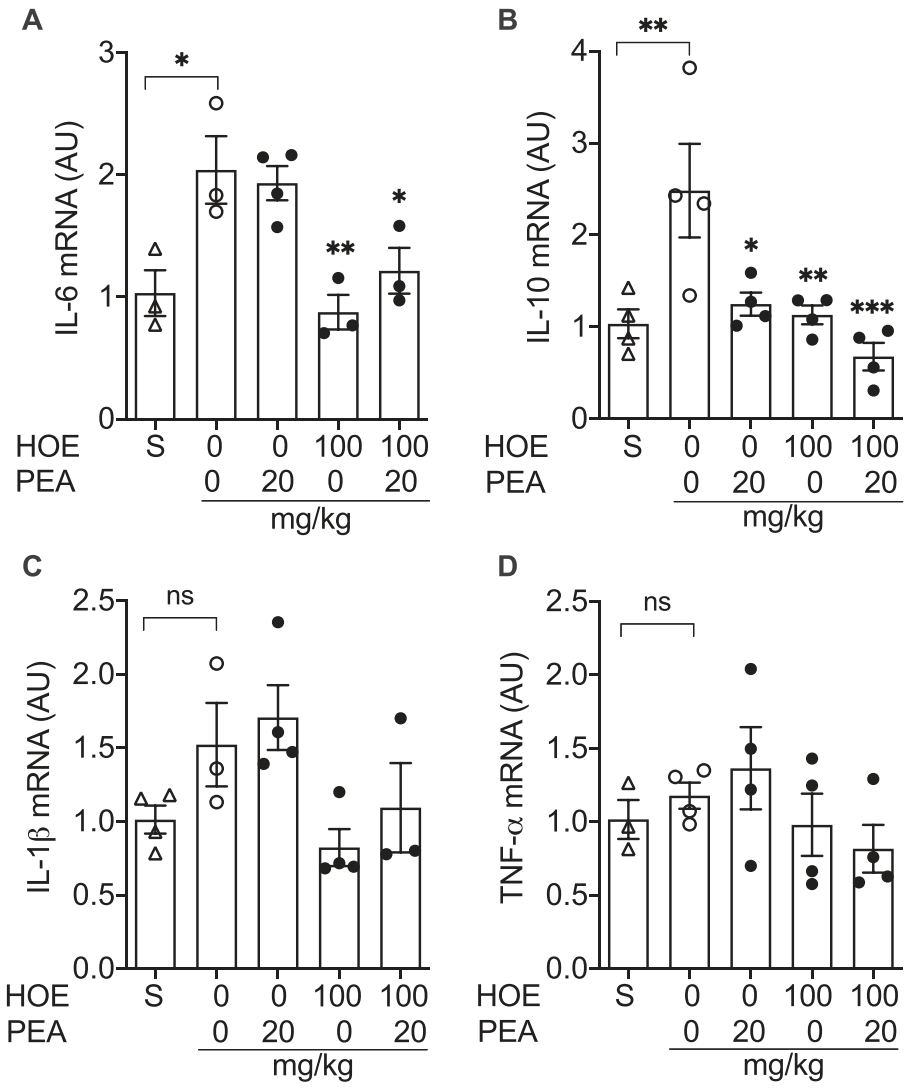

Fig. 7. Effects of HOE (100 mg.kg-1), PEA (20 mg.kg-1) or their combination on mRNA levels (AU, Arbitrary Units) of IL-6 (A), IL-10 (B), IL-1b (C) and TNF-α (D) in lumbar spinal cords (L3-L6). Bars represent mean ± S.E.M. (n = 3–4 per group) and analyzed by oneway ANOVA followed by Dunnett's test for multiple comparisons. $^{*}P < 0.05$, $^{**}P < 0.01$ and $^{***}P < 0.001$ vs. Vehicle. S, sham; ns, non-significant.

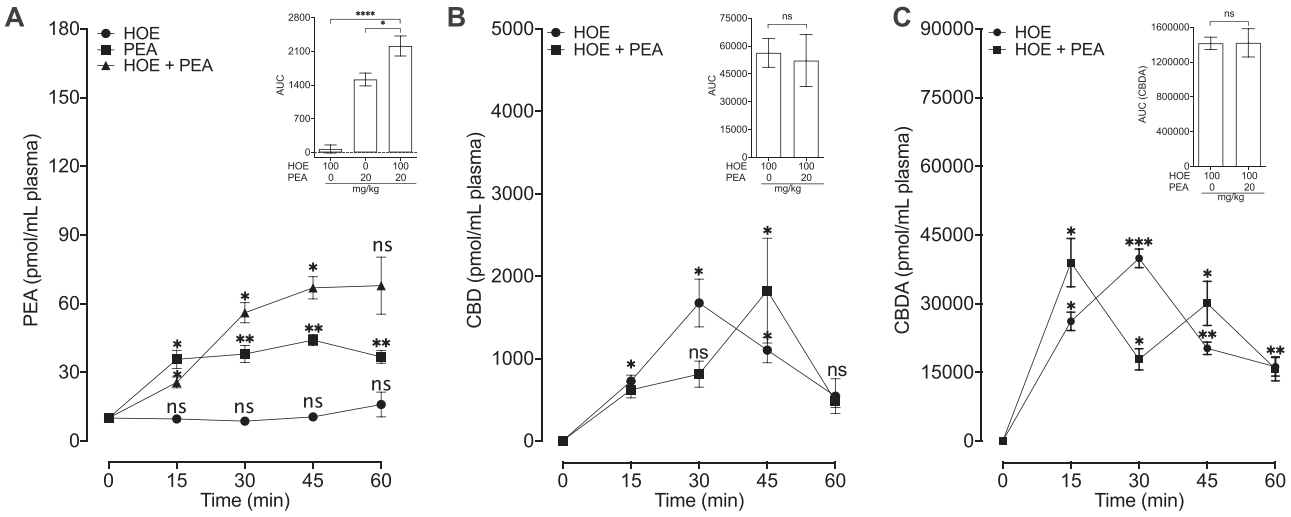

Fig. 8. Concentration-time curves and overall drug exposure (AUC) for PEA (A), CBD (B) and CBDA (C) in mouse plasma, after oral administration of HOE (100 mg.kg-1) alone or in combination with PEA (20 mg.kg-1). Data are expressed as mean ± S.E.M (n = 3–5 per group) and analyzed by one-way ANOVA (AUC curves) and two-way ANOVA (concentration-time curves) followed by Dunnett's test for multiple comparisons. $^{**}P < 0.01$ vs. baseline or combination of HOE plus PEA.

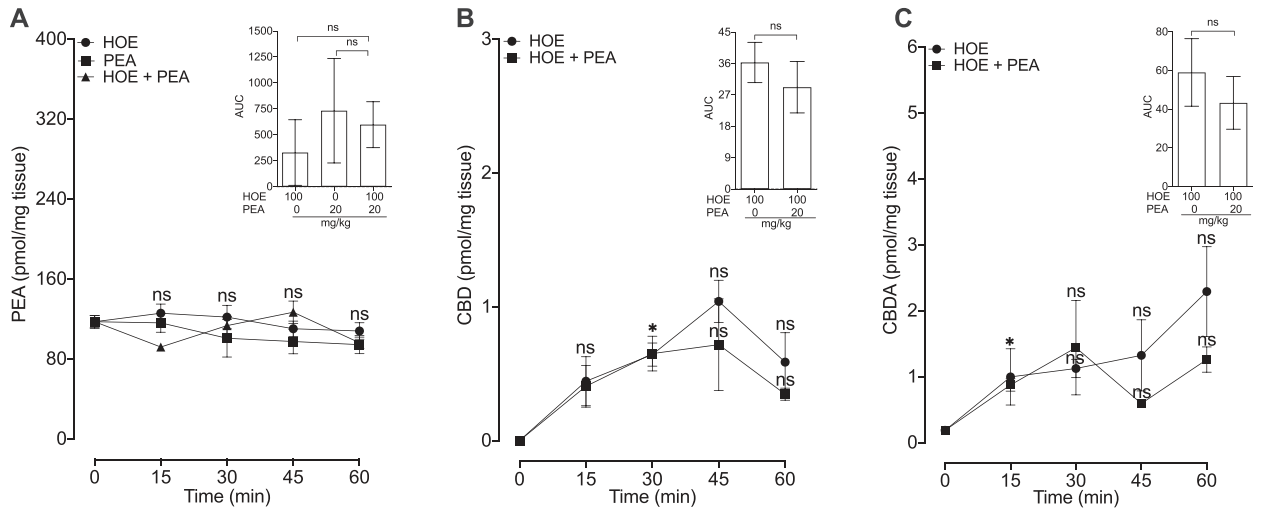

Fig. 9. Concentration-time curves and overall drug exposure (AUC) for PEA (A), CBD (B) and CBDA (C) in lumbar spinal cord tissue, after oral administration of HOE (100 mg.kg-1) alone or in combination with PEA (20 mg.kg-1). Data are expressed as mean ± S.E.M. (n = 3–5 per group) and analyzed by one-way ANOVA (AUC curves) and two-way ANOVA (concentration-time curves) followed by Dunnett's test for multiple comparisons. $^{*}P < 0.05$ vs. baseline or combination of HOE plus PEA.

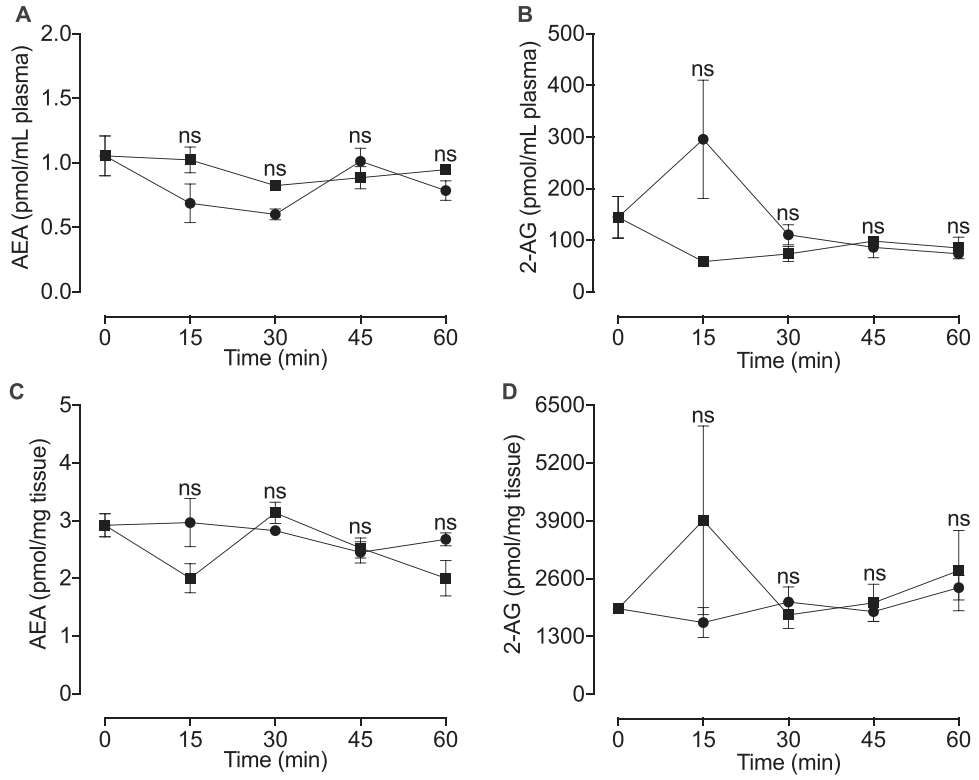

Fig. 10. Time-course of the effects of oral administration of HOE (100 mg.kg-1; •) alone or in combination with PEA (20 mg.kg-1; ■) on the levels of anandamide (AEA) and 2- arachidonoyl-sn-glycerol (2-AG) in mouse plasma (Upper panels) and spinal cords (lower panels). Data are expressed as mean} S.E.M. (n = 3–5 per group) and analyzed by twoway ANOVA followed by Dunnett's test for multiple comparisons.

of HOE, CBD and CBDA. The mechanism underpinning the pharmacokinetic interaction between HOE and PEA is unknown, but two speculative scenarios are worth mentioning. First, HOE could act as a carrier to increase the intestinal absorption of PEA. This is sometimes observed with plant extracts, especially if they contain terpene compounds [48]. Second, HOE could slow down the liver degradation of PEA, which is primarily mediated by FAAH. Evidence in the literature suggests that CBD, which is present in HOE, inhibits FAAH activity at micromolar concentrations [21].

This study has several limitations. First, we used combination subthresholding rather than isobolographic analysis to test the interaction between HOE and PEA. This selection was imposed by the weak effects of HOE, which did not allow us to determine a median effective dose for the compound. Though combination subthresholding is well established, it fails to define the doses at which the combination of HOE/PEA can be expected to have synergistic effects, which can only be addressed

by dose-effect-based approaches [14]. Second, we only investigated male mice. As growing evidence indicates that there are significant sex-related differences in pain responses [27], future work will need to include female animals. To the best of our knowledge, sexual dimorphisms have been observed in the antinociceptive effects of some components of hemp, including CBD [5], but not in the response to PEA. Third, our pharmacokinetic studies were focused on CBD and CBDA, even though many other naturally occurring chemical constituents in HOE may impact the pharmacokinetic properties of PEA. Lastly, the chemical composition of hemp and hemp-derived products varies considerably depending on various factors including growth conditions and extraction methods [29], which may render difficult a head-to-head efficacy comparison across different products.

In conclusion, our findings identify an unexpected synergistic interaction between THC-free hemp and the endogenous analgesic and anti-inflammatory factor PEA, such that the combination of the two compounds exerts greater-than-additive antinociceptive effects in mouse models of acute and chronic pain. This synergism may be at least partially ascribed to the ability of HOE to increase the systemic exposure to PEA after oral administration.

Significance statement

There is an unmet medical need for safe and effective analgesics. Our results suggest that hemp oil extract is modestly effective, when administered alone, in treating acute and chronic pain. Surprisingly, however, the extract strongly enhanced the analgesic effects of palmitoylethanolamide, an endogenous lipid mediator, such that the combination of the two compounds exerted greater-than-additive antinociceptive effects in two mouse models of pain. This synergism may be harnessed therapeutically to produce adequate pain relief without causing undesirable side effects.

CRediT authorship contribution statement

Participated in research design: Piomelli, Mabou Tagne, Fotio and Karimian Azari. Conducted experiments: Mabou Tagne, Fotio, Lin, Squire, Ahmed and Ibne Rashid. Contributed new reagents or analytic tools: Karimian Azari. Performed data analysis: Mabou Tagne and Fotio. Wrote or contributed to the writing of the manuscript: Piomelli, Mabou Tagne and Fotio.

Conflict of interest

Dr. Elnaz Karimian Azari is an employee of Metagenics, which provided financial support for the present study.

Appendix A. Supporting information

Supplementary data associated with this article can be found in the online version at doi:10.1016/j.phrs.2021.105545.

References

[1] J.L. Arruda, S. Sweitzer, M.D. Rutkowski, J.A. Deleo, Intrathecal anti-IL-6 antibody and IgG attenuates peripheral nerve injury-induced mechanical allodynia in the rat: possible immune modulation in neuropathic pain, Brain Res. 879 (1–2) (2000) 216–225, https://doi.org/10.1016/S0006-8993(00)02807-9.

[2] G. Astarita, D. Piomelli, Lipidomic analysis of endocannabinoid metabolism in biological samples, J. Chromatogr. B Anal. Technol. Biomed. Life Sci. 877 (26) (2009) 2755–2767, https://doi.org/10.1016/j.jchromb.2009.01.008.

[3] P.J. Austin, G. Moalem-Taylor, The neuro-immune balance in neuropathic pain: involvement of inflammatory immune cells, immune-like glial cells and cytokines, J. Neuroimmunol. 229 (2010) 26–50.

[4] G.J. Bennett, Y.K. Xie, A peripheral mononeuropathy in rat that produces disorders of pain sensation like those seen in man, Pain 33 (1) (1988) 87–107, https://doi.org/10.1016/0304-3959(88)90209-6.

[5] S.C. Britch, A.G. Goodman, J.L. Wiley, A.M. Pondelick, R.M. Craft, Antinociceptive and immune effects of delta-9-tetrahydrocannabinol or cannabidiol in male versus female rats with persistent inflammatory pain, J. Pharmacol. Exp. Ther. 373 (3) (2020) 416–428, https://doi.org/10.1124/jpet.119.263319.

[6] A. Calignano, G. La Rana, A. Giuffrida, D. Piomelli, Control of pain initiation by endogenous cannabinoids, Nature 394 (6690) (1998) 277–281, https://doi.org/10.1038/28393.

[7] J. Corroon, J.A. Phillips, A cross-sectional study of cannabidiol users, Cannabis Cannabinoid Res. 3 (1) (2018) 152–161, https://doi.org/10.1089/can.2018.0006.

[8] B. Costa, G. Giagnoni, C. Franke, A.E. Trovato, M. Colleoni, Vanilloid TRPV1 receptor mediates the antihyperalgesic effect of the nonpsychoactive cannabinoid, cannabidiol, in a rat model of acute inflammation, Br. J. Pharmacol. 143 (2) (2004) 247–250, https://doi.org/10.1038/sj.bjp.0705920.

[9] B. Costa, A.E. Trovato, F. Comelli, G. Giagnoni, M. Colleoni, The non-psychoactive cannabis constituent cannabidiol is an orally effective therapeutic agent in rat chronic inflammatory and neuropathic pain, Eur. J. Pharmacol. 556 (1–3) (2007) 75–83, https://doi.org/10.1016/j.ejphar.2006.11.006.

[10] V. Curto-Reyes, G. Kirschmann, M. Pertin, S.K. Drexler, I. Decosterd, M.R. Suter, Neuropathic pain phenotype does not involve the NLRP3 inflammasome and its end product interleukin-1β in the Mice spared nerve injury model, PLoS One 10 (7) (2015), e0133707, https://doi.org/10.1371/journal.pone.0133707.

[11] D. De Gregorio, R.J. McLaughlin, L. Posa, R. Ochoa-Sanchez, J. Enns, M. Lopez-Canul, M. Aboud, S. Maione, S. Comai, G. Gobbi, Cannabidiol modulates serotonergic transmission and reverses both allodynia and anxiety-like behavior in a model of neuropathic pain, Pain 160 (1) (2019) 136–150, https://doi.org/10.1097/j.pain.0000000000001386.

[12] P. Dubový, V. Brázda, I. Klusáková, I. Hradilová-Svíženská, Bilateral elevation of interleukin-6 protein and mRNA in both lumbar and cervical dorsal root ganglia following unilateral chronic compression injury of the sciatic nerve, J. Neuroinflamm. (2013) 10, https://doi.org/10.1186/1742-2094-10-55.

[13] D. Dubuisson, S.G. Dennis, The formalin test: a quantitative study of the analgesic effects of morphine, meperidine, and brain stem stimulation in rats and cats, Pain 4 (1977) 161–174, https://doi.org/10.1016/0304-3959(77)90130-0.

[14] J. Foucquier, M. Guedj, Analysis of drug combinations: current methodological landscape, in: Pharmacology Research and Perspectives, 3, Wiley-Blackwell Publishing Ltd., 2015, p. 149, https://doi.org/10.1002/prp2.149.

[15] S. Franchi, A.E. Valsecchi, E. Borsani, P. Procacci, D. Ferrari, C. Zaffa, P. Sartori, L. F. Rodella, A. Vescovi, S. Maione, F. Rossi, P. Sacerdote, M. Colleoni, A.E. Panerai, Intravenous neural stem cells abolish nociceptive hypersensitivity and trigger nerve regeneration in experimental neuropathy, Pain 153 (4) (2012) 850–861, https://doi.org/10.1016/j.pain.2012.01.008.

[16] L. Gabrielsson, S. Mattsson, C.J. Fowler, Palmitoylethanolamide for the treatment of pain: pharmacokinetics, safety and efficacy, British Journal of Clinical Pharmacology (2016) 932–942, https://doi.org/10.1111/bcp.13020.

[17] R. Gallily, Z. Yekhtin, L.O. Hanuš, The anti-inflammatory properties of terpenoids from cannabis, Cannabis Cannabinoid Res. 3 (1) (2018) 282–290, https://doi.org/10.1089/can.2018.0014.

[18] K. Genaro, D. Fabris, A.L.F. Arantes, A.W. Zuardi, J.A.S. Crippa, W.A. Prado, Cannabidiol is a potential therapeutic for the affective-motivational dimension of incision pain in rats, Front. Pharmacol. 8 (2017) 391, https://doi.org/10.3389/fphar.2017.00391.

[19] J. Guindon, J. LoVerme, A. De Léan, D. Piomelli, P. Beaulieu, Synergistic antinociceptive effects of anandamide, an endocannabinoid, and nonsteroidal anti-inflammatory drugs in peripheral tissue: a role for endogenous fatty-acid ethanolamides? Eur. J. Pharmacol. 550 (1–3) (2006) 68–77, https://doi.org/10.1016/j.ejphar.2006.08.045.

[20] D.C. Hammell, L.P. Zhang, F. Ma, S.M. Abshire, S.L. McIlwrath, A.L. Stinchcomb, K. N. Westlund, Transdermal cannabidiol reduces inflammation and pain-related behaviours in a rat model of arthritis, Eur. J. Pain. 20 (6) (2016) 936–948, https://doi.org/10.1002/ejp.818.

[21] F.M. Leweke, D. Piomelli, F. Pahlisch, D. Muhl, C.W. Gerth, C. Hoyer, J. Klosterkötter, M. Hellmich, D. Koethe, Cannabidiol enhances anandamide signaling and alleviates psychotic symptoms of schizophrenia, Transl. Psychiatry 2 (3) (2012), e94, https://doi.org/10.1038/tp.2012.15.

[22] L. Lin, H. Yang, P.J.H. Jones, Quantitative analysis of multiple fatty acid ethanolamides using ultra-performance liquid chromatography-tandem mass spectrometry, Prostaglandins Leukot. Essent. Fat. Acids 87 (6) (2012) 189–195, https://doi.org/10.1016/j.plefa.2012.09.001.

[23] J. Lo Verme, J. Fu, G. Astarita, G. La Rana, R. Russo, A. Calignano, D. Piomelli, The nuclear receptor peroxisome proliferator-activated receptor-α mediates the anti-inflammatory actions of palmitoylethanolamide, Mol. Pharmacol. 67 (1) (2005) 15–19, https://doi.org/10.1124/mol.104.006353.

[24] J. LoVerme, R. Russo, G. La Rana, J. Fu, J. Farthing, G. Mattace-Raso, R. Meli, A. Hohmann, A. Calignano, D. Piomelli, Rapid broad-spectrum analgesia through activation of peroxisome proliferator-activated receptor-α, J. Pharmacol. Exp. Ther. 319 (3) (2006) 1051–1061, https://doi.org/10.1124/jpet.106.111385.

[25] K. Mackie, Cannabinoid receptors as therapeutic targets, Annu. Rev. Pharmacol. Toxicol. 46 (1) (2006) 101–122, https://doi.org/10.1146/annurev.pharmtox.46.120604.141254.

[26] A.M. Malfait, R. Gallily, P.F. Sumariwalla, A.S. Malik, E. Andreakos, R. Mechoulam, M. Feldmann, The nonpsychoactive cannabis constituent cannabidiol is an oral anti-arthritic therapeutic in murine collagen-induced arthritis, Proc. Natl. Acad. Sci. U.S.A. 97 (17) (2000) 9561–9566, https://doi.org/10.1073/pnas.160105897.

[27] J.S. Mogil, Sex differences in pain and pain inhibition: multiple explanations of a controversial phenomenon, in: Nature Reviews Neuroscience, 13, Nature Publishing Group, 2012, pp. 859–866, https://doi.org/10.1038/nrn3360.

[28] T. Murakami, T. Kanchiku, H. Suzuki, Y. Imajo, Y. Yoshida, H. Nomura, D. Cui, T. Ishikawa, E. Ikeda, T. Taguchi, Anti-interleukin-6 receptor antibody reduces neuropathic pain following spinal cord injury in mice, Exp. Ther. Med. 6 (5) (2013) 1194–1198, https://doi.org/10.3892/etm.2013.1296.
[29] D. Namdar, M. Mazuz, A. Ion, H. Koltai, Variation in the compositions of cannabinoid and terpenoids in Cannabis sativa derived from inflorescence position along the stem and extraction methods, Ind. Crops Prod. 113 (2018) 376–382, https://doi.org/10.1016/j.indcrop.2018.01.060.
[30] National Academies of Sciences, E. and M, The health effects of cannabis and cannabinoids: the current state of evidence and recommendations for research, in: Psychiatria, 15, Via Medica, 2017, https://doi.org/10.17226/24625.
[31] S. Petrosino, V. Di Marzo, The pharmacology of palmitoylethanolamide and first data on the therapeutic efficacy of some of its new formulations, in: British Journal of Pharmacology, 174, John Wiley and Sons Inc, 2017, pp. 1349–1365, https://doi.org/10.1111/bph.13580.
[32] D. Piomelli, The endocannabinoid system: a drug discovery perspective, Curr. Opin. Investig. Drugs 6 (7) (2005) 672–679. https://europepmc.org/article/med/16044662.
[33] D. Piomelli, A fatty gut feeling, in: Trends in Endocrinology and Metabolism, 24, Elsevier Current Trends,, 2013, pp. 332–341, https://doi.org/10.1016/j.tem.2013.03.001.
[34] K. Ren, R. Dubner, Interactions between the immune and nervous systems in pain, in: Nature Medicine, 16, Nat Med., 2010, pp. 1267–1276, https://doi.org/10.1038/nm.2234.
[35] E.M. Rock, C.L. Limebeer, L.A. Parker, Effect of cannabidiolic acid and Δ9-tetrahydrocannabinol on carrageenan-induced hyperalgesia and edema in a rodent model of inflammatory pain, Psychopharmacology 235 (11) (2018) 3259–3271, https://doi.org/10.1007/s00213-018-5034-1.
[36] E.B. Russo, Taming THC: potential cannabis synergy and phytocannabinoid-terpenoid entourage effects, Br. J. Pharmacol. 163 (7) (2011) 1344–1364, https://doi.org/10.1111/bph.2011.163.
[37] Ethan B. Russo, Beyond cannabis: plants and the endocannabinoid system, in: Trends in Pharmacological Sciences, 37, Elsevier Ltd., 2016, pp. 594–605, https://doi.org/10.1016/j.tips.2016.04.005.
[38] R. Russo, J. LoVerme, G. La Rana, G. D'Agostino, O. Sasso, A. Calignano, D. Piomelli, Synergistic antinociception by the cannabinoid receptor agonist anandamide and the PPAR-α receptor agonist GW7647, Eur. J. Pharmacol. 566 (1–3) (2007) 117–119, https://doi.org/10.1016/j.ejphar.2007.03.007.
[39] P. Sacerdote, S. Franchi, S. Moretti, M. Castelli, P. Procacci, V. Magnaghi, A. E. Panerai, Cytokine modulation is necessary for efficacious treatment of experimental neuropathic pain, J. Neuroimmune Pharmacol. (2013) 202–211, https://doi.org/10.1007/s11481-012-9428-2. Springer.
[40] J. Scholz, C.J. Woolf, The neuropathic pain triad: neurons, immune cells and glia, in: Nature Neuroscience, 10, Nature Publishing Group, 2007, pp. 1361–1368, https://doi.org/10.1038/nn1992.
[41] K.A.B. Simão da Silva, A.F. Paszcuk, G.F. Passos, E.S. Silva, A.F. Bento, F.C. Meotti, J.B. Calixto, Activation of cannabinoid receptors by the pentacyclic triterpene α,β-amyrin inhibits inflammatory and neuropathic persistent pain in mice, Pain 152 (8) (2011) 1872–1887, https://doi.org/10.1016/j.pain.2011.04.005.
[42] K. Starowicz, D.P. Finn, Cannabinoids and pain: sites and mechanisms of action, in: Advances in Pharmacology, 80, Academic Press Inc., 2017, pp. 437–475, https://doi.org/10.1016/bs.apha.2017.05.003.
[43] M.A. Thacker, A.K. Clark, F. Marchand, S.B. McMahon, Pathophysiology of peripheral neuropathic pain: immune cells and molecules, Anesth. Analg. 105 (3) (2007) 838–847, https://doi.org/10.1213/01.ane.0000275190.42912.37.
[44] G. Varrassi, E. Alon, M. Bagnasco, L. Lanata, V. Mayoral-Rojals, A. Paladini, J. V. Pergolizzi, S. Perrot, C. Scarpignato, T. Tölle, Towards an effective and safe treatment of inflammatory pain: a delphi-guided expert consensus, in: Advances in Therapy, 36, Springer Healthcare, 2019, pp. 2618–2637, https://doi.org/10.1007/s12325-019-01053-x.
[45] V. Vozella, C. Zibardi, F. Ahmed, D. Piomelli, Fast and sensitive quantification of δ9-tetrahydrocannabinol and its main oxidative metabolites by liquid chromatography/tandem mass spectrometry, Cannabis Cannabinoid Res. 4 (2) (2019) 110–123, https://doi.org/10.1089/can.2018.0075.
[46] S. Vučkovic, D. Srebro, K.S. Vujovic, Č. Vučetic, M. Prostran, Cannabinoids and pain: new insights from old molecules, Front. Pharmacol. 9 (2018), https://doi.org/10.3389/fphar.2018.01259.
[47] S.J. Ward, S.D. McAllister, R. Kawamura, R. Murase, H. Neelakantan, E.A. Walker, Cannabidiol inhibits paclitaxel-induced neuropathic pain through 5-HT 1A receptors without diminishing nervous system function or chemotherapy efficacy, Br. J. Pharmacol. 171 (3) (2014) 636–645, https://doi.org/10.1111/bph.12439.
[48] A.C. Williams, B.W. Barry, Penetration enhancers, Adv. Drug Deliv. Rev. 56 (5) (2004) 603–618, https://doi.org/10.1016/j.addr.2003.10.025.
[49] W. Xiong, T. Cui, K. Cheng, F. Yang, S.-R. Chen, D. Willenbring, Y. Guan, H.-L. Pan, K. Ren, Y. Xu, L. Zhang, Cannabinoids suppress inflammatory and neuropathic pain by targeting α3 glycine receptors, J. Exp. Med. 209 (6) (2012) 1121–1134, https://doi.org/10.1084/jem.20120242.
[50] Y.F. Zhu, K. Linher-Melville, M.J. Niazmand, M. Sharma, A. Shahid, K.L. Zhu, N. Parzei, J. Sidhu, C. Haj, R. Mechoulam, G. Singh, An evaluation of the anti-hyperalgesic effects of cannabidiolic acid-methyl ester in a preclinical model of peripheral neuropathic pain, Br. J. Pharmacol. 177 (12) (2020) 2712–2725, https://doi.org/10.1111/bph.14997.